A new setup for analysis of the performance of micropumps for drug delivery

Christine Barrot-Lattes, O. Thuillard, Christine Barrot, Stéphane Colin, Lucien Baldas, Nicolas Laurien, Stéphane Orieux, Jean-Louis Fraysse, Didier Forêt, Frédéric Casanova, et al.

A NEW SETUP FOR ANALYSIS OF THE PERFORMANCE OF MICRO-PUMPS FOR DRUG DELIVERY

Christine Barrot*[1], Stéphane Colin[1], Lucien Baldas[1], Nicolas Laurien[1], Stéphane Orieux[1], Jean-Louis Fraysse[2], Didier Forêt[3], Frédéric Casanova[2], Olivier Thuillart[3], Dan Veale[3]

[1] Université de Toulouse; UPS, INSA; ICA; 135 avenue de Rangueil F-31077 Toulouse, France
christine.barrot@iut-tlse3.fr, stephane.colin@insa-toulouse.fr, lucien.baldas@insa-toulouse.fr, nicolas.laurien@insa-toulouse.fr, stephane.orieux@insa-toulouse.fr

[2]SADIR Assistance, ZAC de la Grande Borde, Voie l'Occitane, BP 87555, 31675 LABEGE CEDEX, jlfraysse@sadir-assistance.com, fcasanova@sadir-assistance.com

[3]Fédération ANTADIR; 66 boulevard Saint-Michel, 75006 Paris
foret@antadir.com, antadir@antadir.com, veale.dan@gmail.com

KEY WORDS

Microfluidics, Microflowrate measurements, Experimental setup, Micropumps

ABSTRACT

This paper presents a new experimental setup for the accurate measurement of micro-flowrates delivered by medical micropumps. It permits measurement of both mean and instantaneous flowrates, which is necessary for evaluating the performance of pulsed micropumps. Typical measured flowrates are in the range of $2.5\times10^{-13} m^3.s^{-1}$ *to* $2.5\times10^{-11} m^3.s^{-1}$*. Two types of measurement are possible : (i) the mean flowrate is obtained by timing the displacement of an air bubble between two optical sensors in a 5µl calibrated micropipette; (ii) an image analysis of bubble displacement tracked by a camera inside the pipette provides instant flowrate. In order to allow continuous testing of micropumps, the setup has been designed to perform an automatic injection of a new bubble as soon as the previous one reaches the outlet of the pipette. The size of the bubble is controlled by adjusting the opening time of a solenoid valve. The system is encased in an insulated chamber equipped for thermal regulation between 283 K and 318 K. An analysis of the measurement uncertainties is described, and typical results obtained for various micropumps are presented and discussed. Pulsed flowrates are observed and they are explained by the specific pumping mechanism of the pumps. The performances of different micropumps are finally discussed for a set of different temperatures.*

1. INTRODUCTION

In the recent years, the improvement in miniaturization techniques has led to the development of many novel systems. New devices are continuously being developed and their numerous applications in medicine or biotechnology need to be accurately tested because of the impact of their performances on humans. For example, drug delivery micro-pumps, without having sub-millimetric dimensions, deliver small volumes of drug with a flowrate in the range of 10^{-6} to 10^{-13} $m^3.s^{-1}$. Verifying the characteristics of such devices poses the problem frequently encountered in microflows studies, of the accurate measurement of the delivered flowrates.

Many flowmeters based on different working principles have been developed, but few are dedicated to very small flowrates i.e. less than 1 $l.h^{-1}$ ($2.78\times10^{-7} m^3.s^{-1}$). The main measurement techniques relative to microflowrates are summarized in the reviews of Schnell [1] , Nguyen [2] or Baldas and Caen [3] :

* Corresponding author

- Liquid / Air interface tracking : an amount of liquid volume per unit of time is measured by following the movement of the gas-liquid interface -or two in the case of bubble tracking- inside a calibrated duct [4, 5, 6]. The volumetric flowrate is measured downstream from the microsystem [7]. The main limitations of this method are (i) variations of the movement of the meniscus due to exterior elements such as dust obstructing the ducts, (ii) measurement errors which can be significant because the position of the meniscus is often manually detected (iii) downstream pressure which should be the atmospheric pressure.
- Fluid weight measurement : this technique which is easy to implement, is widely used [1, 8]. The weight of fluid is measured at the outlet of the channel with a precision electronic balance (with a range on the order of 0.001g to 0.01g). The main disadvantage comes from the evaporation of the tested liquid. Most of the authors neglect this [9], others take it into account in the data processing [10, 11] or put a protection layer on the liquid in the downstream weighted reservoir [12].
- Conduction properties of fluid : this technique consists in deducing the flowrate from the thermal exchanges in the fluid flow. A thermal resistor with a temperature larger than the flow temperature is placed into the flowstream. The generated heat transfer gives rise to a temperature gradient which is measured with sensors downstream and upstream from the warm element [13]. The temperature difference is proportional to the flowrate. Miniaturized flowmeters have been developed [14] and some of them have evolved into commercial products [15]. They can measure flowrates down to 50 $nl.min^{-1}$ ($8.33\times10^{-13}\,m^3.s^{-1}$) but in certain cases, friction forces are too big and prohibit their use. Another drawback is that the flowmeter is dependant to the type of liquid and needs a calibration for each liquid.

In this article, a new experimental setup for microflowrate measurements is presented. Its principle is based on the air bubble tracking method. The first part of this paper is dedicated to the description of the experimental setup and its specificities. The setup permits measurement of both mean and instantaneous flowrates lower than $3\times10^{-10}\,m^3.s^{-1}$. To permit successive flowrate measurements, a special setup has been designed to inject an air bubble automatically. The total system is in an insulated chamber and a thermal control loop allows maintenance of constant thermal conditions during the measurements of the flowrate. To determine the accuracy of the measurements, an uncertainties analysis has been performed. In the second part of the article, typical results obtained with the experimental setup are presented. Flowrates of infusion systems for drug delivery have thus been measured at different working temperatures.

2. EXPERIMENTAL SETUP

2.1. General principle of measurements

The experimental setup (Figure 1) is designed to measure liquid flowrates in the range of $2.5\times10^{-10}\,m^3.s^{-1}$ to $2.5\times10^{-13}\,m^3.s^{-1}$. Two methods of measurement are used simultaneously. The first is based on bubble tracking : an air bubble is pushed by the liquid flow inside a calibrated glass pipette. The flow rate can be deduced from the time interval between the detection of the bubble with two optical sensors mounted on the pipette. This gives a mean flowrate, the pipette volume between the two sensors being 5µl. The second method consists in deducing a flowrate from image analysis. Images of the air bubble are registered by a video camera, the comparison between two successive images in the sequence allows one to obtain the displacement of the bubble inside the pipette and, given the acquisition frequency, and the instantaneous flow rate. According to Bretheton's work [16], the speed of the bubble is assumed to be the same as the velocity of the flowing liquid.
In order to have a succession of measurements, a system permitting the automatic injection of the air bubble into the pipette has been specially designed and is detailed below. The whole system is inserted in an insulated chamber. A thermal control loop coupled with a Peltier module is used for the temperature regulation. All the data are recorded with a PC acquisition system and analyzed using specific software.

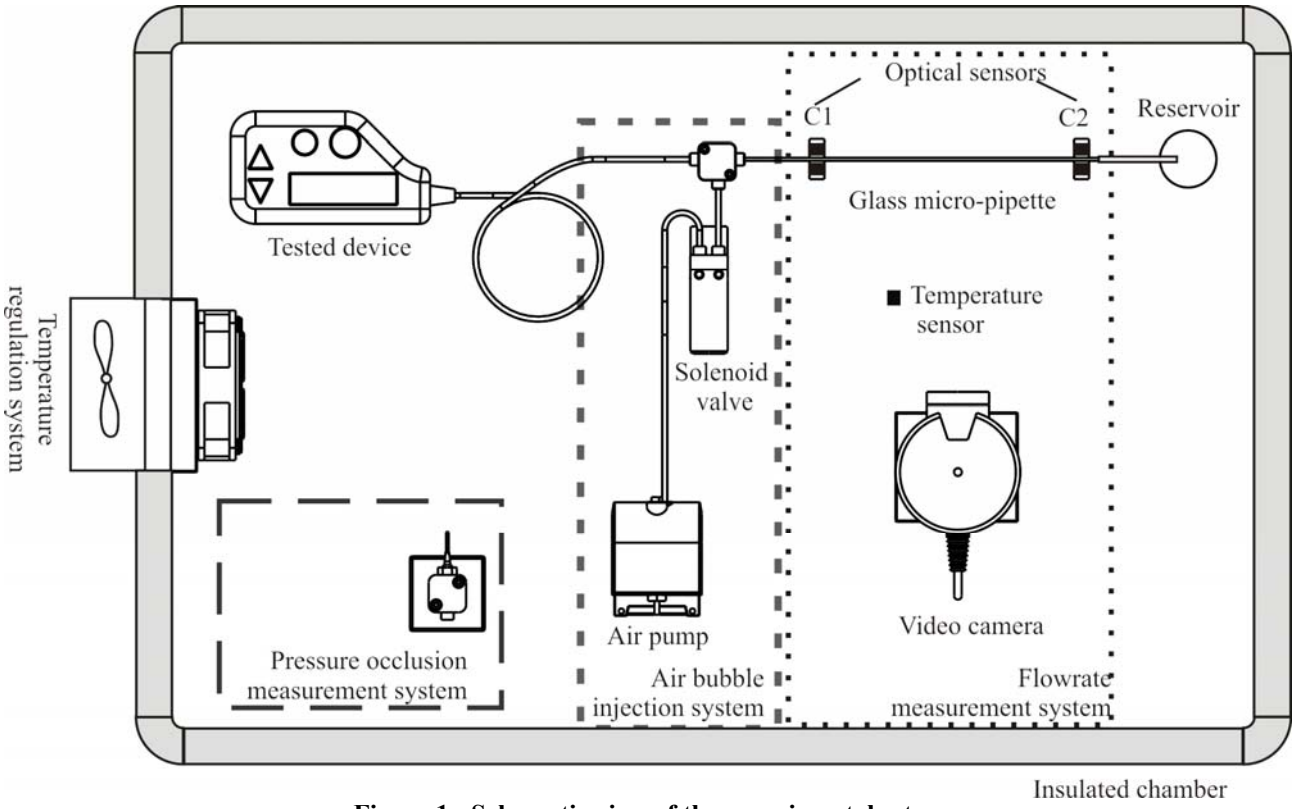

Figure 1 : Schematic view of the experimental setup

2.2. Flowrate measurements and uncertainties evaluation

2.2.1. Global flowrates

a. Optical sensors technique

Between the two sensors seperated by length *l*, the volumetric flowrate $Q_{os} = \partial V / \partial t$ is given by :

$$Q_{os} = \frac{V}{\Delta t} \qquad (1)$$

Where Δt is the time spent by the bubble travelling to from one optical sensor to another and *V* is the displaced volume of liquid, given by :

$$V = l\, A, \qquad (2)$$

A being the cross-sectional area of the calibrated pipette.

The glass micro-pipette is a DURAN® calibrated pipette. The given accuracy of its volume is lower than $\pm 0.3\%$. The measurements of the internal diameter of the pipette, *D*, have been performed with a profile projector on a sample of ten pipettes (Figure 2) with a resolution of $\pm 2\,\mu m$. The pipettes have been cut at different lengths. The mean measured diameter is 289.6 µm with a standard deviation of 2.19µm. The resulting relative standard measurement uncertainty on the diameter, is then 0.85%.

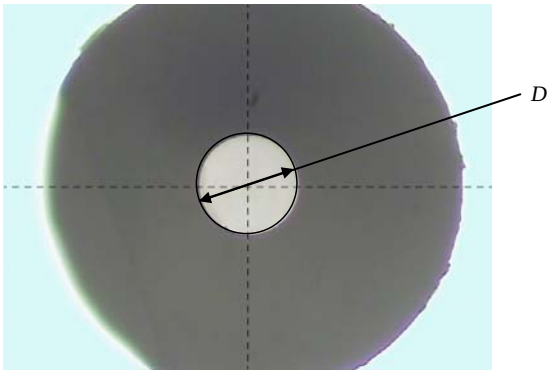

Figure 2 : Cross-section of the pipette: image obtained with a profile projector

The distance between the two sensors l has been measured using a numeric micrometric table with a displacement resolution of 0.1 mm. In order to be the same conditions as during the experiments, an air bubble has been blocked in the pipette. The optical sensors have been fixed and the inter-distance was evaluated in moving the pipette and recording the change in the sensor signal due to the passage of the front and the rear menisci of the bubble (Figure 3). The average distance obtained between the two sensors is 74.3 mm with a standard deviation of 0.25 mm. The relative uncertainty is then near 0.4 %.

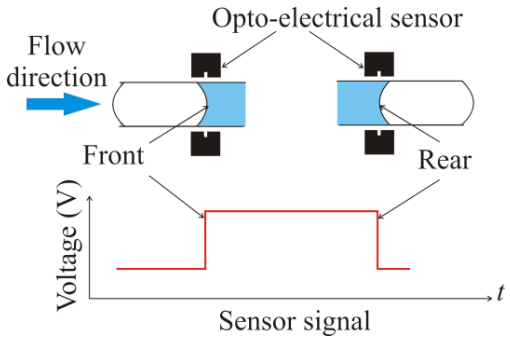

Figure 3 : Optical sensor - principle of bubble detection

Therefore, the total uncertainty on the volume of fluid between the two sensors can be calculated as follows :

$$\frac{\Delta V}{V} = \frac{\Delta l}{l} + \frac{\Delta A}{A} = \frac{\Delta l}{l} + 2\frac{\Delta D}{D} \qquad (3)$$

and is equal to : $\Delta V / V = 0.4 + 2 \times 0.85 = 2.1\%$ which is also the uncertainty of the flowrate Q_{os} .

The two interfaces of the air bubble permit a double measurement of the flowrate: one for the front meniscus, one for the rear meniscus.

b. Image analysis technique

A serie of images are recorded with a video camera (1.3Mpixels). The frequency of acquisition, f, is adapted to the flowrate and (in the range of 0.5 to 60 frames per second) in order to have a displacement of the bubble between two images not smaller than 10 pixels. For each image of the sequence, the positions of the front and the rear menisci are recorded in pixels with a precision of ± 2 pixels. In order to take into account the camera distortion, the images are cut out in zones as it is shown in Figure 4.

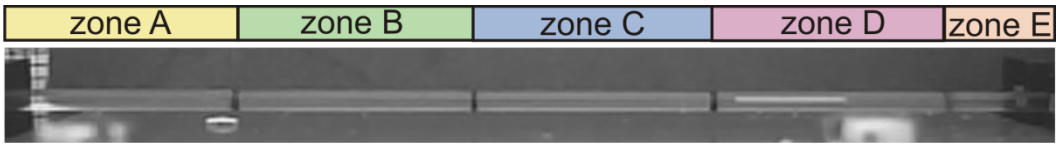

Figure 4 : Typical recorded image and delimitation of the zones (above)

The length of each zone is measured with a micrometer, and a specific scale factor k_i *(i=A,…,E)* is calculated as the ratio of the length in millimeters over the length in pixels for each zone. The position of the meniscus in millimeters, P , can be deduced with the following equation :

$$P = k \times p \,, \qquad (4)$$

where p is the position of the meniscus in pixels. The uncertainty of P can be evaluated to ± 0.3 mm taking into account the uncertainty of k ($\pm 1\%$) and the uncertainty of p. A linear fitting of the positions of the front and the rear menisci (Figure 5) allows one to obtain the velocity of the bubble (slope of the curve) with a precision of $\pm 0.5\%$. The volumetric flowrate Q_{ia} obtained with image analysis is :

$$Q_{ia} = v\, A \qquad (5)$$

where v is the velocity of the meniscus. The error made on this measure is estimated as follows :

$$\frac{\Delta Q_{ia}}{Q_{ia}} = \frac{\Delta A}{A} + \frac{\Delta v}{v} = 2\frac{\Delta D}{D} + \frac{\Delta v}{v} \qquad (6)$$

and is equal 2.2 %.

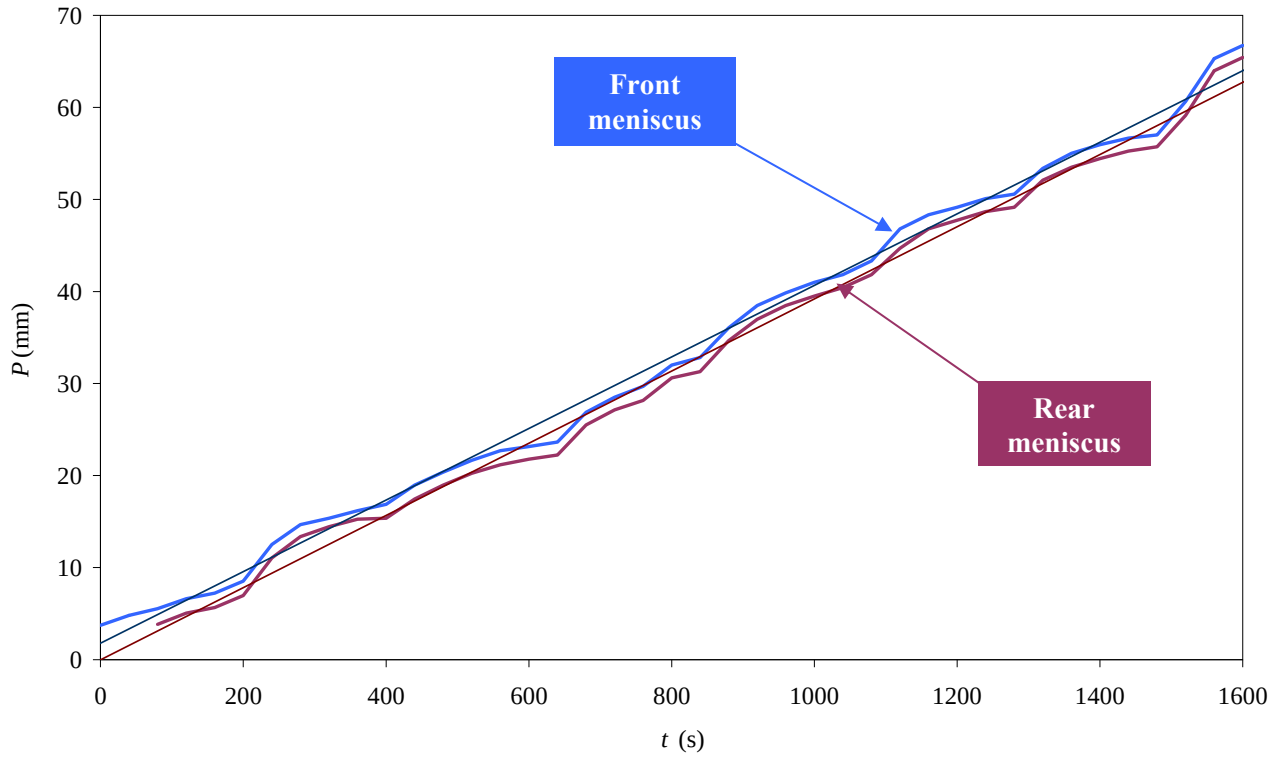

Figure 5 : Typical position evolution of front meniscus (–) and the rear meniscus (–) of the bubble Micropump Flowrate 10 mm^3/h – 303 K

As an example, the velocities obtained with the measurement plotted in Figure 5 are 0.0387×10^{-3} m.s^{-1} for the front meniscus and 0.0392×10^{-3} m.s^{-1} for the rear meniscus, the respective resulting volumetric flow rates being 9.2 ± 0.4 mm^3.h^{-1} and 9.28 ± 0.4 mm^3.h^{-1}.

2.2.2. Instantaneous flowrate

An instantaneous volumetric flowrate, Q_i, is also obtained by image analysis according to the following equation :

$$Q_i = f\ A\, d \qquad (7)$$

where f is the image acquisition frequency, d is the displacement of the bubble between two successive images and A the cross-section area of the glass pipette. Two flowrates can be calculated, one from the front meniscus, the other from the rear meniscus displacement. This data processing allows one to follow the temporal evolution of the flowrate and to highlight particularities in the behaviour of tested device. Nevertheless, the quantitative information must not be taken into account because it depends on the time step chosen.

An example of drug delivery micropump instantaneous flowrate is shown in Figure 6. The irregularities observed come from the design of the tested pump. The peak in flowrate with the constant periodicity of 180 seconds is due to the step motor of the pump.

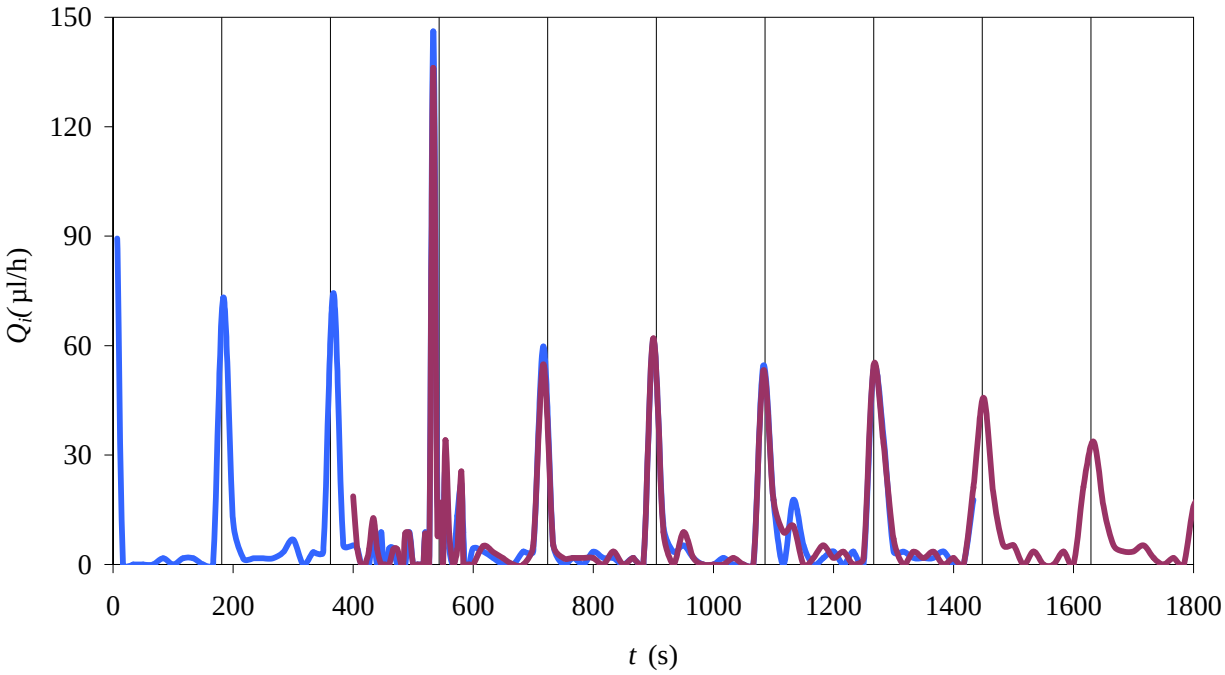

Figure 6 : Instantaneous flowrate (–) front meniscus, (–) rear meniscus - Micropump Flowrate 10 mm^3/h – 303 K

Another advantage of this method is the possibility to validate each measurement : the control of the size the of the bubble permits checking of its behavior (dissolution, division) during the experiment.

2.3. Thermal regulation

The whole experimental device is in an insulated chamber whose walls are in Plexiglas and lined with an insulating material. A temperature sensor PT100 (with 0.15 °C resolution) permits measurement of the temperature variation inside the chamber. A thermal control loop with a Peltier module regulates the temperature inside the chamber in the range of 483 K to 318 K. Figure 2 shows a typical temperature recorded inside the chamber over 1500s. The set temperature is 313 K, the mean temperature obtained is 313 K with a standard deviation of 0.5%.

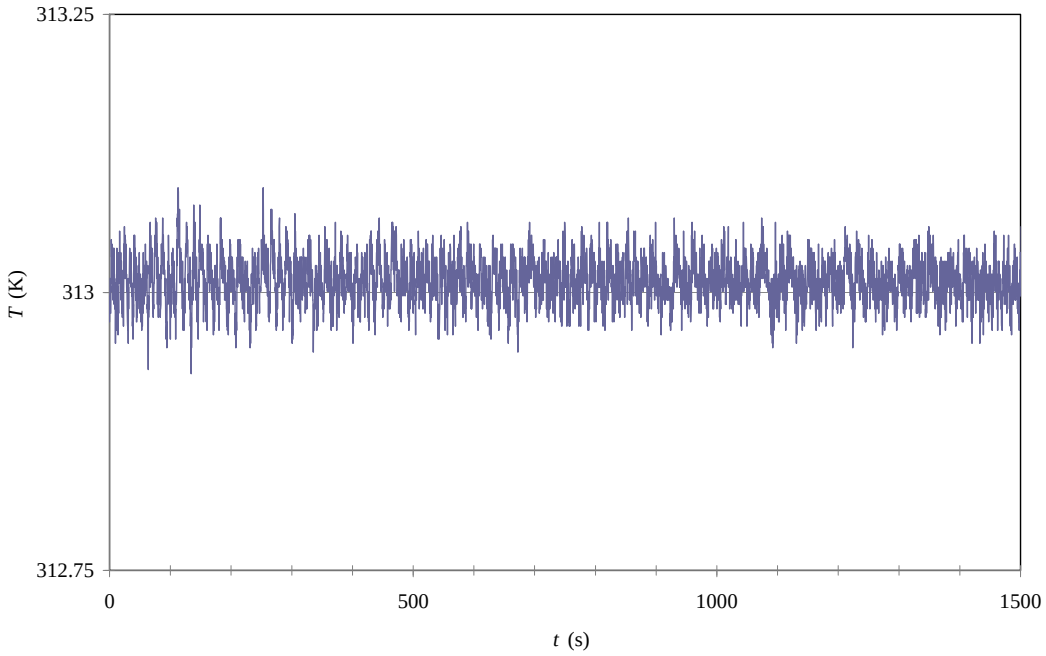

Figure 7 : Typical temperature evolution in the chamber

2.4. Air bubble injection

For very slow flowrates, the measurement time corresponding to the time elapsed by the bubble between one sensor and another can reach several hours. For example, for a flowrate of $2\times10^{-13}m^3.s^{-1}$, the experiment takes at least 5 hours. To be able to do a series of measurements without any manual intervention, a special setup has been designed and manufactured in order to have an automatic injection of the bubble. The micro-bubble generation system is a stainless steal T-junction. (Figure 8).

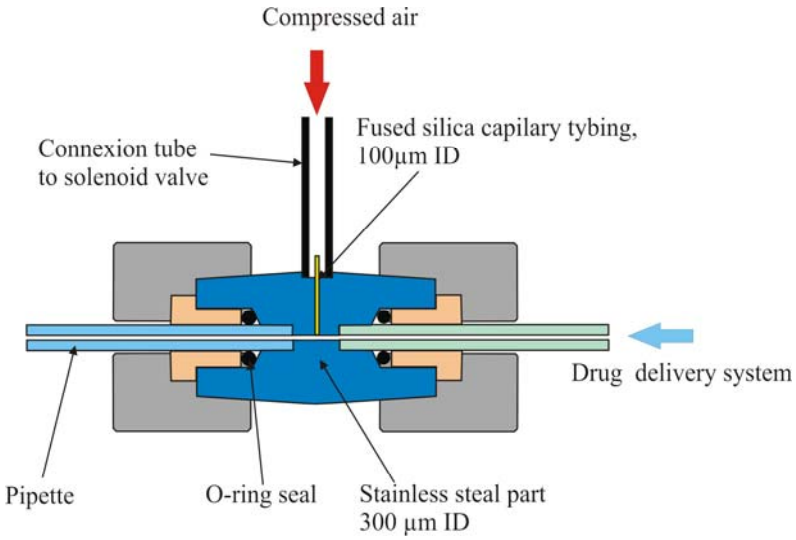

Figure 8 : Schematic view of the micro bubble generation system - Inside view of the T-junction

The flow of the liquid phase comes directly from the outlet of the micropump via a catheter connected to the junction. The liquid goes through a main channel whose diameter is 300 µm in order to minimize both the dead space volume and the changes in cross-section. The bubble is introduced into the main flow by means of a fused silica secondary channel with an internal diameter of 100µm. This dimension avoids a back flow of liquid in the capillary tubing. As can be seen in Najafi & al. [17] (Figure 9), air pressure must be applied to create an air bubble in the liquid phase. In our case, this is done by mean of a pump that can deliver an air pressure of 2000 Pa.

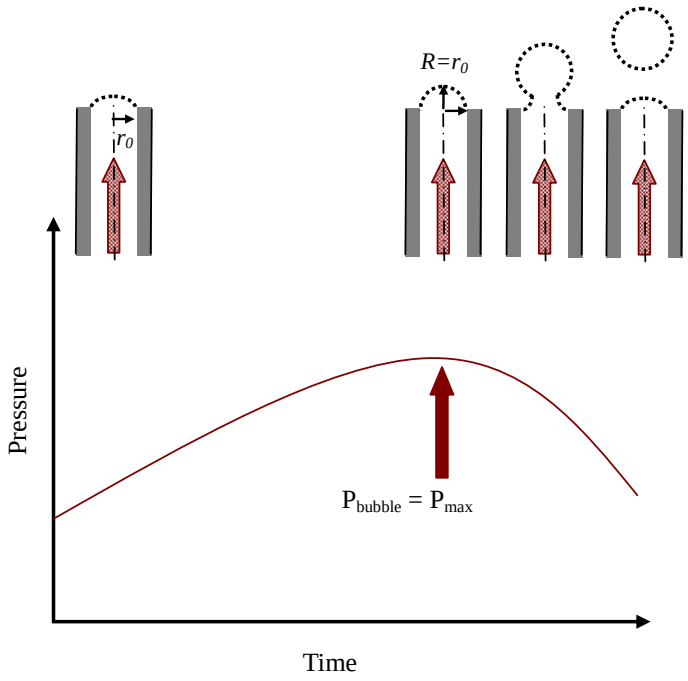

Figure 9 : Bubble generation process and pressure variation with time from [16]

The automatic generation of a new bubble is controlled by a PC and an acquisition card according to the following process : when a bubble is at the outlet of the pipette, a solenoid valve is opened and a new bubble is introduced. To adjust the bubble length, the opening time of the valve and the air pressure are controlled. Initial tests have been performed in order to verify the repetitivity of the setup. In Figure 10, the lengths of seven successive bubbles are presented, the opening time of the valve was 500 ms and the air pressure was 4500 Pa. The length varies from 10mm to 16mm, with a mean length of 14mm. These variations can be explained by irregularity in the flowrate delivered by the micropump : the liquid pressure inside the T-junction is not constant, changing the conditions of bubble generation.
An optimization of these parameters is currently under study, the goal being to have a length of 10 mm whatever the flowrate. The air pump is then replaced by a compressed air system, a pressure regulator and a manometer that are used to control and measure the air pressure.

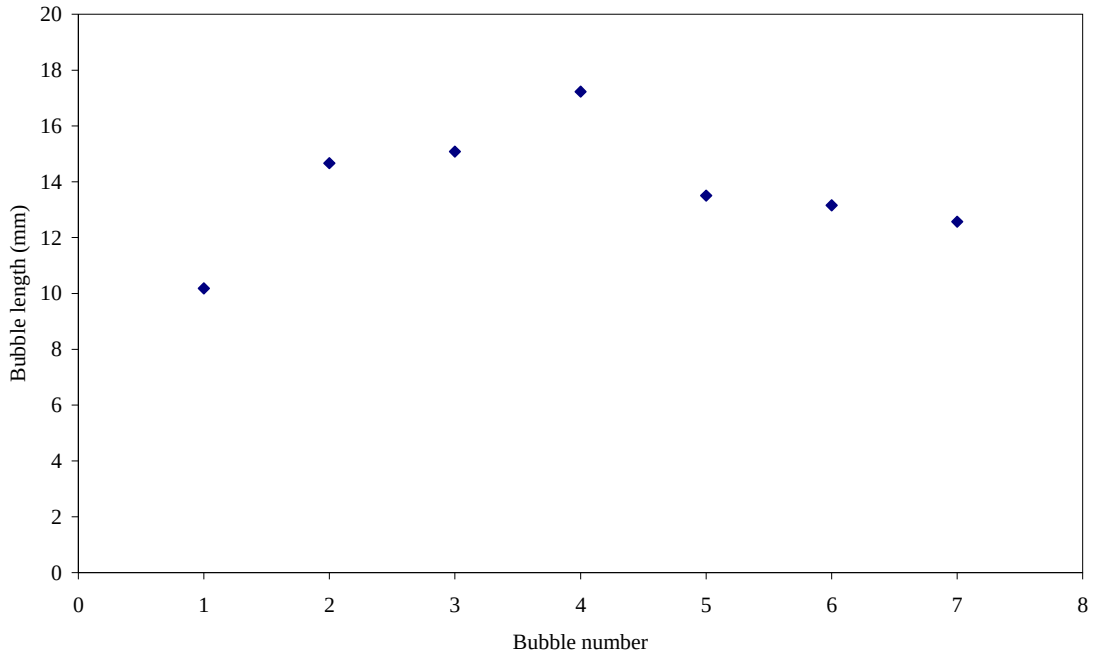

Figure 10 : Bubble lengths obtained in a succession of six bubbles - Opening time of the valves : 500 ms, air pressure : 4500 Pa

3. FLOWRATE MEASUREMENTS OF A DRUG DELIVERY MICROPUMP

Initial experiments have been on drug delivery micropumps. They were conducted with various flowrates : 100 mm^3/h, 10 mm^3/h and bolus (for which the value is not indicated by the manufacturers) at different temperatures. The optical sensor technique was used first. The results are presented in Figures 11, 12 and 13. The flowrate tends to decrease when the temperature increases. A possible explanation is the dilatation of elements of the micropump (plastic syringe or catheter).

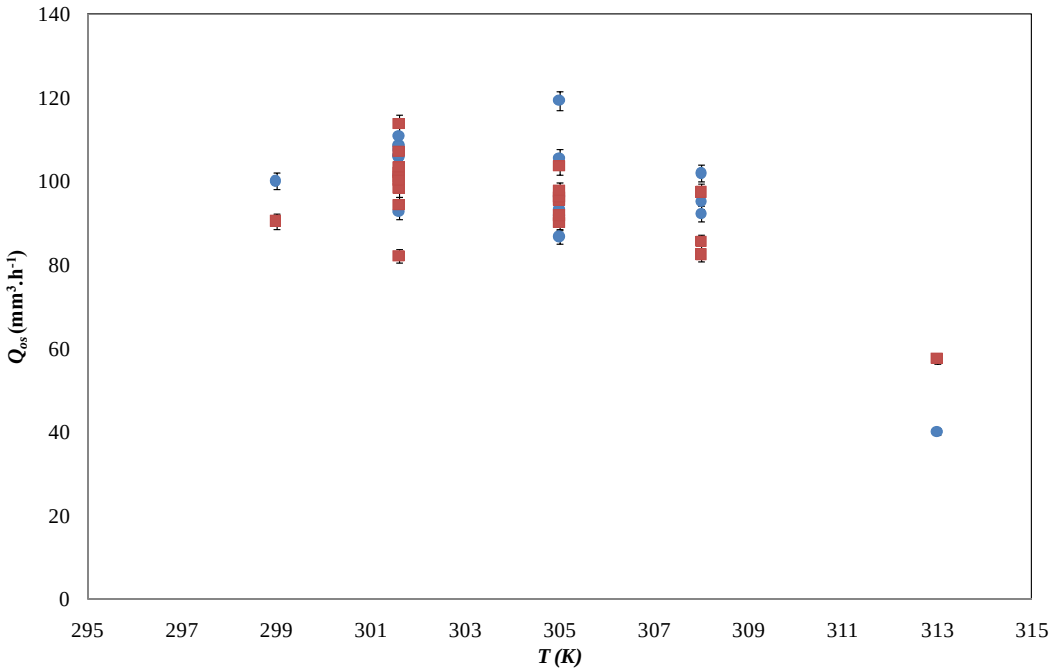

Figure 11 : Flowrates obtained with optical sensor technique at different temperatures : 299K, 301 K, 305 K, 308 K and 313 K – (■) Front meniscus (●) Rear meniscus – Micropump setup flowrate : 100mm^3.h^{-1}

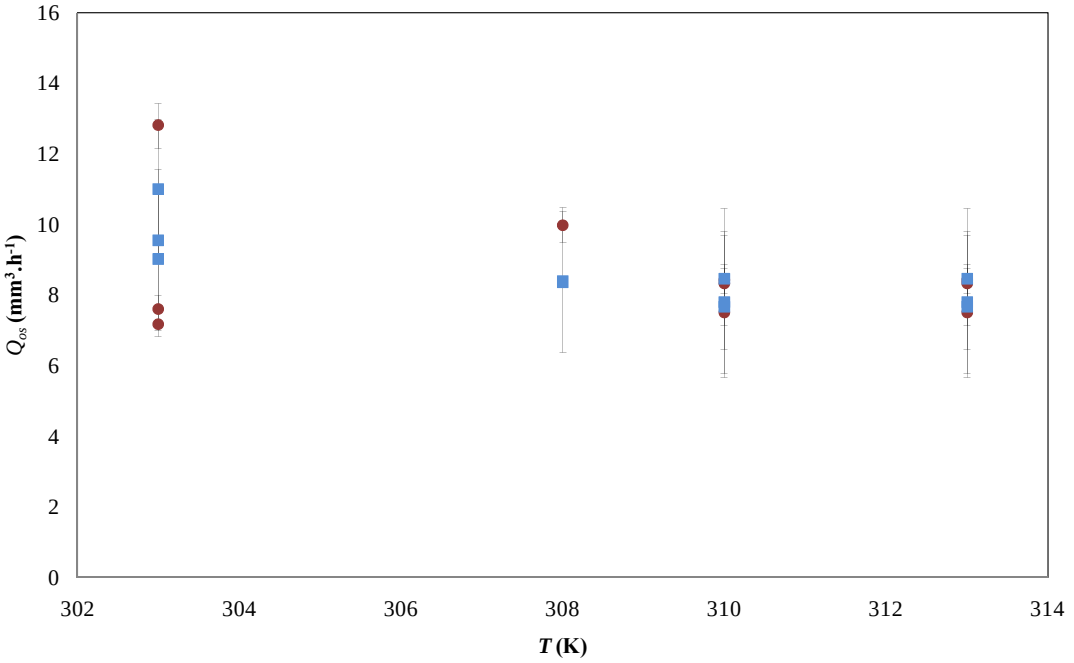

Figure 12 : Flowrates obtained with optical sensor technique at different temperatures : 303 K, 308 K, 310 K and 313 K – (■) Front meniscus (●) Rear meniscus – Micropump setup flowrate : 10mm^3.h^{-1}

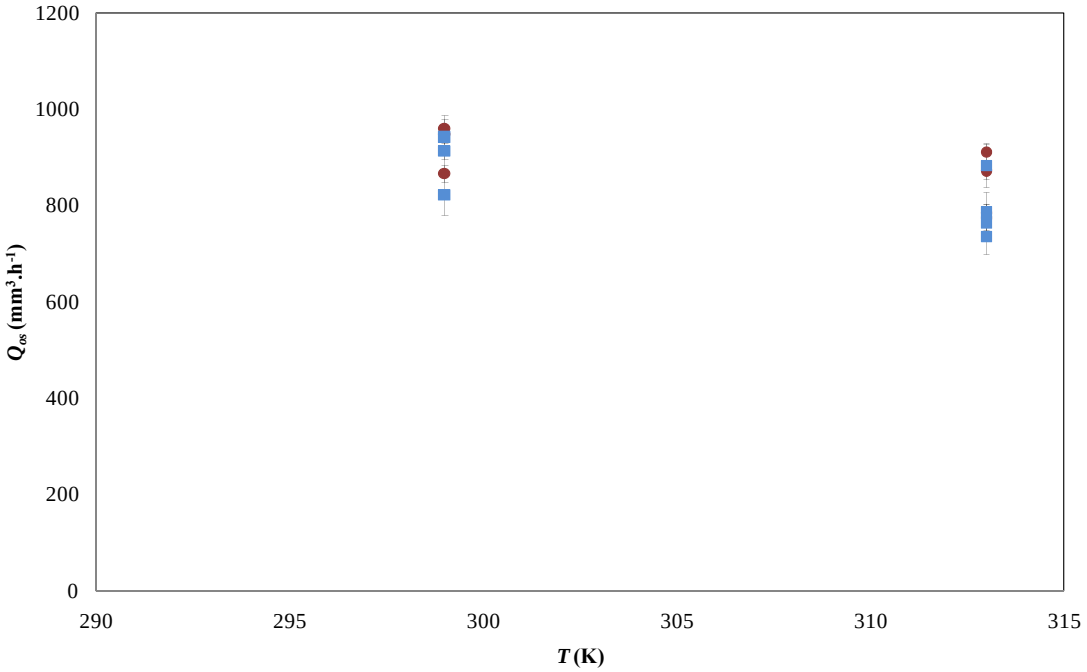

Figure 13 : Flowrates obtained with optical sensor technique at different temperatures : 299 K and 313 K – (■) Front meniscus (●) Rear meniscus – Micropump setup flowrate : Bolus (1000mm^3.h^{-1})

Another observation is the dispersion of the results : for a given temperature, the dispersion of the flowrate values can reach 10% of the flowrate value. That can be explained by the design of the micropump. As shown in Figure 6, the behavior of the stepper motor is periodic. The volume of the glass pipette around 5 mm^3 does not allow smoothing of the peaks of flowrates during the measurements.
Complementary tests have been carried out to determine the number of samples necessary to obtain a mean delivered flowrate (Figure 14). Seventy consecutive air bubbles have been generated for the experiments. For each, the flowrate has been calculated by the optical sensor method. The mean flowrate and the standard deviation value versus the number of values are plotted in Figure 6. They become constant for more than 40 samples.

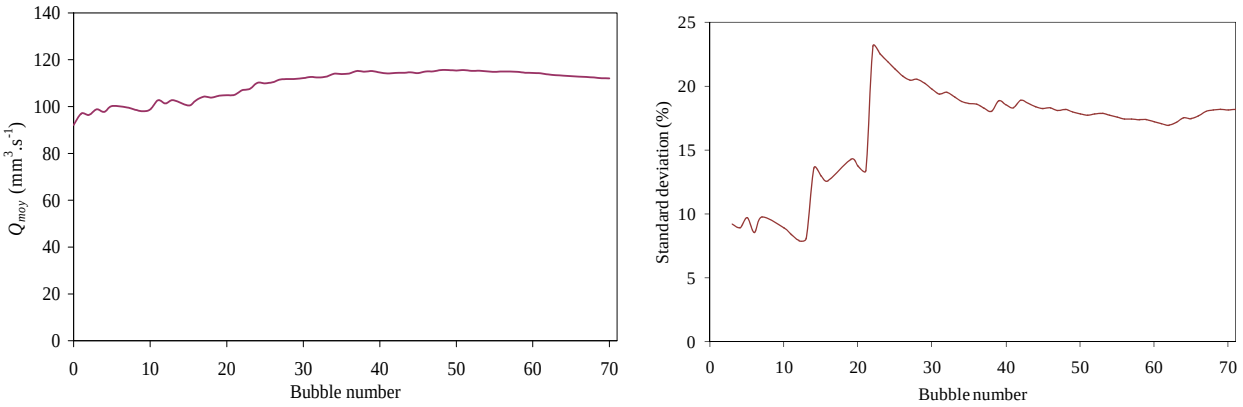

(a) **(b)**

Figure 14 : Convergences of (a) mean flowrate and (b) standard deviation in function of the number of bubbles – Optical sensor technique - Front meniscus data – Setup flowrate on micropump : 100mm^3.s^{-1}

4. CONCLUSIONS AND PERSPECTIVES

The description of a new experimental setup for micro-flowrate measurements has been presented. The range of measured flowrate is 2×10^{-13} to 2×10^{-11} $m^3.s^{-1}$, with an uncertainty of the measurement near $\pm 2\%$. It is based on a bubble tracking technique : one measure is obtained with optical sensors; the second is deduced from image analysis. The main advantages of this setup are

- The small volume of fluid needed for the measurements (milliliters);
- The double measurement of flowrate using two methods;
- The automatic operation that does not require manual intervention for series of measurements;
- Thermal regulation : the setup is in an insulated chamber, the temperature range is 283 K-318 K.

The measurements of flowrates delivered by a micropump for drug delivery are presented. Flowrate fluctuations of flowrate are observed; they are due to the design of the micropumps. A temperature dependence of the flowrate is also observed and needs additional investigations.

NOMENCLATURE

A	Cross-section area of calibrated pipette, m^2
D	Internal diameter of glass pipette, m
d	Displacement of bubble, m
f	Image acquisition frequency, Hz
k	Scale factor, $mm.pixel^{-1}$
l	Distance between opto-electrical sensors, m
p	Meniscus position, *pixels*
P	Meniscus position, mm
Q_i	Instantaneous flowrate, $m^3.s^{-1}$
Q_{ia}	Volumetric flowrate obtained by image analysis, $m^3.s^{-1}$
Q_{moy}	Mean volumetric flowrate, $m^3.s^{-1}$
Q_{os}	Volumetric flowrate obtained by optical sensor technique, $m^3.s^{-1}$
r_0	Fused silica capillary radius, m
R	Bubble radius, m
t	Time, s
V	Volume, m^3

REFERENCES

[1] Schnell, G. (1997). Measurement of very small liquid flows. *Experimental Thermal and Fluid Science*, **15**, n°4, 406-412.

[2] Nguyen, N. (1997). Micromachined flow sensors--a review. *Flow Measurement and Instrumentation*, **8**, n°1, 7-16.

[3] Baldas, L., Caen R. (2010). Chap. 7 : Experimental Methods in *Microfluidics*, S. Colin. 303-348.

[4] Anduze, M. (2000). Etude expérimentale et numérique de micro-écoulements liquides dans les microsystèmes fluidiques. PhD, Institut National des Sciences Appliquées de Toulouse.

[5] Renaud, L., Malhaire, C., Kleimann, P., Barbier, D., Morin, P. (2008). Theoretical and experimental studies of microflows in silicon microchannels. *Materials Science and Engineering: C*, **28**, n°5-6, 910-917.

[6] Richter, M., Woias, P., Wei, D. (1997). Microchannels for applications in liquid dosing and flow-rate measurement. *Sensors and Actuators A: Physical*, **62**, n°1-3, 480-483.

[7] Pfahler, J., Harley, J., Bau, H., Zemel, J. (1991). Gas and liquid flow in small microchannels. *Symposium on Micromechanical Sensors, Actuators, and Systems*, **32**, 49-60.

[8] Xu, B., Ooti, K.T., Wong, N.T., Choi, W.K. (2000). Experimental investigation of flow friction for liquid flow in microchannels. *International Communications in Heat and Mass Transfer*, **27,** n°8, 1165-1176.
[9] Ren, L., Qu, W., Li, D. (2001). Interfacial electrokinetic effects on liquid flow in microchannels. *International Journal of Heat and Mass Transfer*, **44**, n°16, 3125-3134.
[10] Judy, J., Maynes, D., Webb, B.W. (2002). Characterization of frictional pressure drop for liquid flows through microchannels. *International Journal of Heat and Mass Transfer*, **45**, n°17, 3477-3489.
[11] Kohl, M., Abdel-Khalik, S., Jeter, S., Sadowski, D. (2005). An experimental investigation of microchannel flow with internal pressure measurements. *International Journal of Heat and Mass Transfer*, **48**, n°8, 1518-1533.
[12] Brutin, D., Tadrist, L. (2003). Experimental friction factor of a liquid flow in microtubes. *Phys. Fluids*, **15**, n°3, 653.
[13] Lötters, J. (2005). Liquid flow sensor for nano- and micro-flow ranges. *Sensor Review*, **25**(1), 20-23.
[14] Piotto, M., Dei, M., Bruschi, P. (2009). Low pressure drop, CMOS compatible liquid flow sensor with sub ml/h resolution. *Procedia Chemistry*, **1**, n°1, 96-99.
[15] Sensirion.(2003). CMOSens technology. US Patent 6813944. www.sensirion.com
[16] Bretherton, F.P. (1960). The motion of long bubbles in tubes. *Journal of Fluid Mechanics*, **10**, 166-188.
[17] Najafi, A.S., Xu, Z., Masliyah, J. (2008). Single micro-bubble generation by pressure pulse technique. *Chemical Engineering Science*, **63**, n°7, 1779-1787.